Differences in leaf and wood traits predict phenological sensitivity to daylength more than temperature

Deirdre Loughnan[1], Faith A M Jones[1], and E M Wolkovich[1]

January 28, 2024

[1] Department of Forest and Conservation, Faculty of Forestry, University of British Columbia, 2424 Main Mall Vancouver, BC Canada V6T 1Z4.

Corresponding Author: Deirdre Loughnan deirdre.loughnan@ubc.ca

Introduction

Climate change is having profound effects on ecological communities, influencing species fitness, interactions, and community structure. Recent shifts in phenologies—the timing of life history events—have been cited as evidence of climate change impacts, with widespread advances being observed across the tree of life (Root et al., 2003; Parmesan and Yohe, 2003). These general phenological response, however, average over high variability across species (Thackeray et al., 2016; Cohen et al., 2018; Kharouba et al., 2018), posing a challenge to accurate forecasts. Understanding what drives this variation is critical to accurately predict future changes in community dynamics and ecosystem services, including pollination and carbon sequestration (Cleland et al., 2007).

In plants, species variation can in part be explained by differences their strategies of growth, which are generally inferred from traits (Violle et al., 2007). Decades of research on plant traits have worked to build predictive models of species responses to the environment (Green et al., 2022), which could be promising to explain species-level variability in phenological responses. Phenology, however, has generally be excluded from plant trait research, making it difficult to leverage this important framework to explain phenological variation and improve predictions.

Variation in traits can arise from differences in environmental drivers at both proximate and ultimate scales. Proximate drivers include local short-term environmental factors, such as temperature, soil moisture, and daylength, that can alter observed plant traits, like the rate of plant growth, or leafout phenology (Menzel et al., 2006). But environmental factors at other spatial and temporal scales may also act as ultimate drivers of variation. For example, temperature variation across the growing season in temperate systems can produce greater abiotic stress early in the season through high risks of frost events. If many species avoid this risk by leafing out later, this variation could also produce greater biotic stress later in the season through a more competitive environment. These ultimate drivers may thus determine how species respond to environmental cues and the effects of biotic interactions to shape species ecological niche and local species assemblages. Collectively how these proximate and ultimate drivers act on a given species shape their phenotype.

Research on trait ecology has illustrated the ways in which species phenotypes correlate with their growth strategies and responses to environments. The consistency in these relationships across communities allows trait values to provide inferences of growth strategies and community processes independent of species identity (McGill et al., 2006). In plants this has led to the development of frameworks, including the leaf economic spectrum (Wright et al., 2004) and wood economic spectrum (Chave et al., 2009). Under these frameworks, trait values follow distinct gradients that range from acquisitive strategies—with plants producing cheaper tissue and overall faster growth—to conservative strategies—under which plants invest in long-lived tissue but grow at slower rates (Wright et al., 2004; Díaz et al., 2016). These traits serve as proxies for difficult to measure physiological processes and responses to biotic interactions (Shipley et al., 2016), but can still provide considerable insights into the mechanisms shaping plant communities globally.

Drawing on the relationships between traits and species growth strategies can potentially further our understanding of how plant communities assemble. To date, many studies have focused on community-level responses, using metrics of functional diversity or community weighted means (such as classic work by Grime, 1974). But these methods fail to account for the high degrees of intraspecific variation across traits (Albert et al., 2010) and are limited in their ability to account for the diversity of factors that lead to trait variation, like changes in species abundance across populations (Hawkins et al., 2017; Peres-Neto et al., 2017; Miller et al., 2019). To best understand the processes that define species strategies, we much account for variation at multiple scales—from proximate to ultimate drivers—and use analytical methods that can accurately partition variance across its many sources.

Phenology itself is considered a trait with high inter- and intra-specific variability. Previous studies have found high variation in phenology for the same species when observed over different years or sites (Primack et al., 2009; Chuine et al., 2010). This variability is often given as justification for excluding phenology from broader functional trait frameworks. But given the importance of phenology in defining species temporal niches and the environmental conditions of growth periods, phenological variation may correlate with other functional traits along the axis of acquisitive to conservative growth strategies.

Understanding whether phenology fits within major functional trait frameworks, however, requires understanding its high variation within species. Phenological variation is generally observed in natural conditions where considerable differences in the major environmental cues that trigger many phenological events—temperature and daylength (Chuine, 2000; Körner and Basler, 2010)—vary across space and time. However, phenology is often highly predictable when decomposed into these underlying environmental cues (Laube et al., 2014). Within-species variation may also occur across other plant traits (e.g., leaf and wood structure traits), which may vary across latitudinal (Wiemann and Bruce, 2002) or environmental gradients (Pollock et al., 2012), though generally to a smaller scale compared to phenology. While our previous growth chamber study found no evidence that phenological cues varied spatially (Loughnan and Wolkovich, in prep), previous work in functional traits has found other traits to exhibit stronger spatial variation in response to gradients in environmental cues (Gross et al., 2000; Wright et al., 2003). These results suggest understanding how phenology and other traits correlate across species will require methods to incorporate variation within species.

Here, we address this challenge using the phenological event of spring budburst alongside a suite of traits that can capture acquisitive to conservative growth strategies (Wright et al., 2004; Reich, 2014). Our study spans across species—including functional groups in both the understory and canopy layers—of temperate deciduous forests in North America, and also across populations within each species. Environmental conditions across the spring in these forests create strong gradients in frost risk, soil nutrients, and light availability, in addition to differences in biotic interactions, such as decreased herbivore apparency and increased competition. We thus predict that these differences between early and late season conditions will select for variation in species growth strategies and as a result, correlate with woody plant traits. We predict that species that grow early in the spring will budburst before canopy closure and have traits we associate with acquisitive growth—particularly shorter heights, small diameters at breast height (DBH), with lower investment in wood density and leaf tissue (low stem specific density and leaf mass area), but greater photosynthetic potential (high leaf nitrogen content

(LNC)). In contrast, we predict species with later budburst will include canopy species that express more conservative growth strategies—exemplified by their greater investments in tissue, with taller heights, large DBH, greater SSD and LMA, but low LNC.

We decompose high phenological variation in budburst date by estimating phenological cues using experiments, then combine multiple sources of variation using a joint modeling approach. We estimate the three major phenological cues for woody plant budburst: two temperature cues—chilling (associated with cool winter temperatures) and forcing (associated with warm spring temperatures) and daylength. These cues correlate with early to late phenology with early species (which we predict have acquisitive traits) showing weaker responses to temperature and daylength, while later species (which we predict have conservative traits) showing stronger responses. Using a powerful joint-modeling approach, we estimate the effects of other plant traits on phenological responses to cues, while partitioning the variance from species- and population-level differences. This approach represents a considerable advance in how we estimate trait-cue relationships, and may allow us to better estimate species phenological responses from available trait data.

Materials and Methods

Field sampling

We combined *in situ* trait data with budburst data from two growth chamber cutting experiments conducted across eastern and western temperate deciduous forests in North America. Both suites of data were collected from populations that span a latitudinal gradient of 4-6° for the eastern and western communities respectively. Our trait measurements were taken across eight populations, of which there were four eastern populations—Harvard Forest, Massachusetts, USA (42.55°N, 72.20°W), White Mountains, New Hampshire, USA (44.11°N, 52.14°W)), Second College Grant, New Hampshire, USA (44.79°N, 50.66°W), and St. Hippolyte, Quebec, Canada (45.98°N, 74.01°W), and four western population—E.C. Manning Park (49.06°N, 120.78°W), Sun Peaks (50.88°N, 119.89°W), Alex Fraser Research Forest (52.14°N, 122.14°W), and Smithers (54.78°N, 127.17°W), British Columbia (BC), Canada (Fig. 1). For the growth chamber studies on budburst phenology, cuttings were collected from the most southern and northern populations in each transect (n_{pop}=4).

Across all eight populations, we measured a diverse assemblage of species from the understory and canopy layers. We selected the angiosperm species that were most abundant, with an aim to maximize the number of closely related species and congeners between our eastern and western communities. We focused on angiosperm species only, as they are more likely to have similar environmental controls to their leafout phenology, and to standardize our leaf trait comparisons by excluding gymnosperms.

Functional traits

We measured all traits in the summer prior to each growth chamber study. For our eastern transect, traits were measured from 8-25 June 2015, and from 29 May to 30 July 2019 for our western transect. At each population, we measured a total of five traits: height, diameter at breast height (DBH), stem specific density (SSD), leaf mass area (LMA), and the percent leaf nitrogen content (LNC). Each trait was measured for each species present at a population, resulting in us measuring 1-10 healthy adult individuals per species at each population. We also used the WSL xylem database (Schweingruber and Landolt, 2010) to collect data on species ring-type for the 72.3% of our species represented in the database.

We measured traits in accordance to the methods discussed by Pérez-Harguindeguy et al. (2013). We calculated tree height using trigonometric methods, using a TruePulse 200L rangefinder and measured DBH 1.37 m from the ground. For shrub heights, we measured the distance from the ground to the height of the top foliage and measured stem diameters at approximately 1 cm above ground-level. To measure stem specific density, we collected a 10 cm sample of branch wood, taken close to the base of the stem. All samples were kept cool during transport and measurements of stem volume taken within 12 hours of sample collection using the water displacement method. We dried our stem samples upon returning from the field at 105°C for 24h, and weighed their dry mass. Stem specific density was calculated as the dry mass of the sample over its fresh volume.

For our two leaf traits, we haphazardly selected five, fully expanded, and hardened leaves, avoiding leaves with considerable herbivory damage. We kept leaves cool during sampling and transport. For each leaf, we took high resolution scans using a Canon flatbed scanner (CanoScan Lide 220) within 12 hours of collection, and estimated leaf area using the ImageJ software (version 2.0.0). Upon returning from the field, we dried our leaves for 48 h at 70°C and weighed each leaf using a precision balance. Leaf mass area was calculated as the ratio of the leaf dry mass over its area. To measure the percent leaf nitrogen content, leaf samples were ground to a find powder and encapsulated for combustion elemental analysis.

Growth chamber study

For our growth chamber study, we collected branch cuttings from our highest and lowest latitude populations in each transect. In both our eastern and western controlled environment study, we included two temperature treatments and daylength, for a total of eight distinct treatments. Our treatments included two levels of chilling—with our eastern study having no additional chilling or 30 days at 4°C, and our western study 30 days or 70 days of chilling at 4°C, with all non-field chilling occurring under dark conditions. Our forcing treatments included either a cool regime of 15:5°C or a warm regime of 20:10°C, and our photoperiod treatments consisted of of either 8 or 12 hour daylengths. We recorded budburst stages of each sample every 1-3 days for up to four months, defining the day of budburst as the day of budbreak or shoot elongation (defined as code 07 by (Finn et al., 2007)). For a more detailed discussion of study sample collection and methods see Loughnan and Wolkovich (in prep).

Statistical Anlaysis

Our analysis combined our *in situ* trait data with budburst data from the controlled environment. For each trait, we developed a joint Bayesian model, in which the relationship between traits and cues is used to estimate budburst. This statistical approach improves upon previous analyses of multiple traits, as it allows us to carry through uncertainty between trait and phenology data—and is better at partitioning the drivers of variation in species phenologies

Our joint model consists of two parts. The first is a hierarchical linear model, in which we have partitioned the variation of individual observations (i) of a given trait value ($y_{\text{trait}[i]}$) to account for the effects of species (*sp id*), population-level differences arising from transects (*transect id*), as well as the interaction between transects and latitude (*transect* $\times$ *latitude*), and finally, residual variation or 'measurement error' (σ_{trait}).

$$\begin{aligned}\mu_{trait} &= \alpha_{\text{grand trait}} + \alpha_{\text{sp[sp id]}} + \beta_{\text{transect}} \times transect + \beta_{\text{transect}\times\text{latitude}} \times (transect \times latitude) \\ \alpha_{sp} &\sim normal(0, \sigma_{sp}) \\ y_{trait} &\sim normal(\mu_{trait}, \sigma_{trait})\end{aligned} \tag{1}$$

Transect was included as a categorical variable and latitude as a continuous variable in our model. Traits were modeled using natural units, with the exception of LMA, which was rescaled by 100 for numeric stability in the model. While each of our traits collected at the individual level were run using separate models, comparisons across species ring-porosity were made using the posterior estimates of our height model. This allowed us to best account for inherent differences in wood anatomy across species and growth form.

We used partial pooling to uniquely estimate species-level variance ($\alpha_{\text{sp[sp id]}}$)—which controls for variation in the number of trait estimates per species and trait variability—which are then used as predictors of species-level estimates of each cue ($\beta_{\text{chill[sp]}}$, $\beta_{\text{force[sp]}}$, $\beta_{\text{photo[sp]}}$).

$$\begin{aligned}\beta_{\text{chill[sp]}} &= \alpha_{\text{chill}[sp]} + \beta_{\text{trait.chill}} \times \alpha_{\text{trait sp[sp]}} \\ \beta_{\text{force[sp]}} &= \alpha_{\text{force}[sp]} + \beta_{\text{trait.force}} \times \alpha_{\text{trait sp[sp]}} \\ \beta_{\text{photo[sp]}} &= \alpha_{\text{photo}[sp]} + \beta_{\text{trait.photo}} \times \alpha_{\text{trait sp[sp]}}\end{aligned} \tag{2}$$

In addition to the species-level estimates, the second part of our model estimates the overall effect of each trait on each cue ($\beta_{\text{trait.chill}}$, $\beta_{\text{trait.force}}$, $\beta_{\text{trait.photo}}$). From this we can estimate how well traits explain species-level differences—by estimating the the species-level cue variation not explained by traits ($\alpha_{\text{chill}[sp]}$, $\alpha_{\text{force}[sp]}$, $\alpha_{\text{photo}[sp]}$) and individual species responses to cues (C_i, F_i, P_i, respectively). Finally, our model estimates the residual budburst variation across species ($\alpha_{\text{pheno[sp]}}$), observations ($\sigma_{\text{pheno}}$), as well as the variation in cues not attributed to the trait (using partial pooling).

$$\begin{aligned}\mu_{pheno} &= \alpha_{\text{pheno[sp]}} + \beta_{\text{chill[sp]}} \times C_i + \beta_{\text{force[sp]}} \times F_i + \beta_{\text{photo[sp]}} \times P_i \\ y_{\text{pheno[i]}} &\sim normal(\mu_{pheno}, \sigma_{\text{pheno}})\end{aligned} \tag{3}$$

$$\begin{aligned}\alpha_{\text{pheno}} &\sim normal(\mu_{\alpha_{\text{pheno}}}, \sigma_{\alpha_{\text{pheno}}}) \\ \alpha_{\text{force}} &\sim normal(\mu_{\alpha_{\text{force}}}, \sigma_{\alpha_{\text{force}}}) \\ \alpha_{\text{chill}} &\sim normal(\mu_{\alpha_{\text{chill}}}, \sigma_{\alpha_{\text{chill}}}) \\ \alpha_{\text{photo}} &\sim normal(\mu_{\alpha_{\text{photo}}}, \sigma_{\alpha_{\text{photo}}})\end{aligned} \tag{4}$$

We included chilling as chill portions, and each environmental cue as continuous variables. We standardized all cues by z-scoring them, allowing us to make comparisons across cues (see Loughnan and Wolkovich (in prep) for more details).

For our model, we used weakly informative priors unique to each trait. We validated our choice of priors using prior predictive checks. All models were coded in the Stan programming language for Bayesian models using the rstan package (Stan Development Team, 2018) in R version 4.3.1 (R Development Core Team, 2017). Each model had four chains, with models run for 6000-8000 total sampling iterations. All our models met basic diagnostic checks, including no divergences, high effective sample sizes (n_{eff}) that exceeded 10% of the number of iterations, and $\hat{R}$ values close to 1. Our model estimates are reported as the mean values, with the 90% uncertainty interval. Estimates are given to one decimal place, as this best represents the level of precision we can infer from our data (Gelman et al., 2020).

Results

Across our eight populations, we measured 47 species of which 28 were in our eastern transect and 22 in our western transect. These include species dominant in both the understory and canopy layer, with our eastern community consisting of 13 shrubs and 15 trees, our western community consisting of 18 shrubs and 4 trees, and three species that occurred in both transects. In total we measured traits of 1428 unique individuals between the two transects across our five traits: height ($n = 1317$), DBH ($n = 1220$), SSD ($n = 1359$), LMA ($n = 1345$), LNC ($n = 1351$). Across our two growth chamber studies, we made observations of 4211 samples, with our observations of budburst spanning 82 and 113 days for our eastern and western studies respectfully.

Most of our traits showed negligible variation across populations, both in terms of differences between the two transects (main effect of transect only) or by latitude within each transect (an interactive effect between transect and latitude). Only leaf mass area (LMA) differed by latitude within transects (0.3, UI: 0.2,0.4, Table 4)—with the LMA of eastern species increasing with latitude—but not western species (Fig. 2 d). Leaf nitrogen content (LNC) and structural traits, however, showed no differences across populations or transects (Table 2 - 3). The differences we found across populations were small to negligible, especially in comparison to species-level differences, which varied considerably and up to 33 fold (Fig. 3).

Only a subset of our traits related to at least one budburst cue, but responses were generally weak, with the exception of trait-specific relationships to photoperiod. We found similar cue relationships for our two structural traits, with tall plants with larger DBH exhibiting stronger photoperiod responses and producing earlier estimates of budburst under longer daylengths (-1.7, UI: -2.9, -0.5 for height and -2.3, UI: -3.4, -1.1 for DBH). But we found no relationship between cues and SSD (Table 3) or between cues and species different types of wood porosity (Fig. 4). Of our two leaf traits, only LMA showed a relationship with photoperiod, with low LMA species advancing their budburst timing more in response to longer photoperiods compared to high LMA species (-7.5, UI: -10.9, -4.1). But we found no relationship between LNC or any of our other cues.

How our three cues shaped budburst timing also varied across our traits. For most of our trait models chilling, followed by forcing, were the strongest cues of budburst (Fig. 5). But in accounting for the correlations between LMA and cues, our model estimated stronger responses to photoperiod (-7.5, UI: -10.9, -4.1) than forcing (-7.1, UI: -13.0, -1.6), and a relatively weak effect of chilling (90% UI crossing zero) (Table 4). In contrast, our LNC (Table 5) and SSD models (Table 3) both showed negligible relationships between photoperiod and budburst timing (90% UI crossing zero). These findings suggest that relationships with additional traits can alter the effects and relative importance of cues on budburst (Fig. 6). This—paired with strong species-level variation—may cause variation in the estimated order of species relative budburst dates across the different models.

In synthesizing the effects of multiple traits across species, our results can be used to make generalizations across ecologically important groups of species. But only some of our models estimated clear gradients in species timing between trees and shrubs (Fig. 7). In particular, we found height to have strong correlations between budburst timing and trait values, with earlier estimates of budbust for shrubs—especially under stronger cues—and later budburst estimates for trees (Fig. 7). Diameter at breast height showed similar trends as estimates from our height model (results not shown). But this was not the case for our two leaf traits. Leaf nitrogen content, for example, showed no distinct separation between shrub and tree functional groups (Fig. 7).

Discussion

Our study combined trait data with phenological cue responses for the same individuals across a large area to understand if phenology fits within a larger trait framework of acquisitive to conservative growth strategies. Of the six traits we studied, we found three that related to phenological cues, but only two of those traits fit within our hypothesized growth paradigm. Using our joint modeling approach, we were able to estimate how these traits interact with cues to shape species budburst timing. We found that photoperiod—often the weakest cue to budburst timing (Laube et al., 2014; Zohner et al., 2016; Flynn and Wolkovich, 2018)—may be the most important cue in trait-phenology relationships. In general, these patterns were consistent across our populations and between our eastern and western transects, despite the differences in latitudes and community composition. Collectively our results provide new insights into the complexity in the mechanisms that underlie the relationships between phenotypes and environmental cues, while also challenging our existing understanding of these processes.

Across our eight forest populations, only one of our varied between our eastern and western communities or with latitude. Overall the observed patterns in leaf mass area (LMA) were in line with our predictions based on the transect differences in species composition. We predicted western communities would express more acquisitive growth strategies on average because they consist of a greater number of shrub species. This was confirmed by the lower LMA we observed in our western transect. This trait differences provide weak support of our predictions that our western deciduous forests differ in their resource partitioning and nutrient cycles based on the traits of their dominant species, despite the fact the dominant shrubs species are more likely to utilize resources early in the season prior to canopy closure.

While the strong differences in our community assemblages explained some of the trait variation we observed spatially, at the species-level the relationships between traits and budburst cues only partially supported our predictions for how phenology relates to species overall growth strategies. Three of our six traits depicted responses to temperature and daylength that followed our predicted correlation with other traits across a gradient of growth strategies. While we predicted species with acquisitive traits—particularly small trees with low stem densities, and leaves with low LMA, and high LNC—to have early budburst via weak temperature and daylength responses, we only found traits to correlate with the effects of daylength on budburst. As predicted, conservative species with greater heights and DBH did have stronger photoperiod responses (associated with later budburst), but—contrary to our prediction—conservative species with high LMA also showed weak responses to photoperiod. These results suggest that phenology is only partially aligns with trends found in established trait frameworks, but also offer new insight into potential tradeoffs in how varying physiological processes shape species temporal niches.

Despite our study spanning forest communities across North America, we found only specific traits to vary spatially. This was surprising, as we expected the inherent variation in temperature and daylengths to impose population differences in species traits. However, research using the similar plant traits have also found little variation in trait values across similar regional scales (Messier et al., 2010; Kang et al., 2013; Standen and Baltzer, 2023). Most of our predictions for how traits pertain to species growth strategies are based on the synthesis of globally distributed species (Wright et al., 2004; Díaz et al., 2016). As such, our findings suggest the importance of studying ecological processes across spatial scales, as the ultimate and proximate drivers selecting species phenotypes appear to vary considerably.

In comparing our results with a global meta-analysis of tree trait relationships with budburst cues (Loughnan et al., in prep), we found similar trait-cue relationships for several of our traits. In addition to also finding relationships between tree height and photoperiod, we found similar responses in leaf traits, with high specific leaf area (the inverse of LMA) exhibiting strong responses to photoperiod (Loughnan et al., in prep). The consistency of this result, across these two spatial scales of study, suggest there are alternate underlying mechanisms shaping how species respond to photoperiod cues. It is possible that the unexpected trends we observed in our results are due to selection on other physiological processes, as many of our traits are associated with one or more ecological function (Wright et al., 2004; Pérez-Harguindeguy et al., 2013; Reich, 2014). The trends we observed in LMA, for example, suggest that selection shaping this trait does not pertain to leaves light capturing abilities, but rather other processes, such as tissue lifespan or decomposition rates (De La Riva et al., 2016).

How traits shape species temporal niches

Individuals temporal niches are shaped by numerous—and complex—interactions with local environmental conditions and species assemblages. But studies that focus only on phenology fail to account for interactions between other traits and cues that also contribute to species temporal niches. In focusing solely on phenology, previous research has shown budburst timing is primarily driven by temperature, with photoperiod being the weakest cue (Chuine et al., 2010; Basler and Körner, 2014; Laube et al., 2014). In contrast with this previous work, we did not find traits to correlate with responses to temperature, suggesting other cues are impacting leaf and structural traits in temperate forests. These traits may relate to other environmental cues known to select for other tree growth events. Soil moisture and changes in water use and cell turgor are known to shape radial growth phenology and shoot elongation in woody plants (Cabon et al., 2020; Peters et al., 2021). Traits like leaf mass area can vary with soil moisture, with variation in leaf area allowing plants to reduce evaporation, selecting for high LMA under dry conditions (De La Riva et al., 2016). If decreases in soil moisture correlate with long photoperiod conditions, it may be contributing to the unexpected trends we observed in LMA and the absence of relationships with temperature. Thus, fully understanding how species growth strategies correlate with phenology may require considering additional cues that are known to shape other plant traits.

Using functional traits to predict climate change responses

Our results offer novel insights into how broader correlations between plant trait syndromes and phenological cues can help predict phenological responses in plant communities with climate change. As temperatures rise, particularly at higher latitudes (Hoegh-Guldberg et al., 2018), these cues will become stronger and potentially select for earlier growth in some species, but photoperiod cues will remain fixed. This suggests the relationships between photoperiod and other traits have the potential to limit species abilities to track temperatures and may constrain the extent to which woody plant phenologies will advance with climate change. Our results suggest that these effects will likely be stronger on larger species or canopy trees and species with relatively low LMA. These constraints could have cascading effects on forest communities, as variable species responses to increasing temperatures further alter species temporal niches and their interactions within communities.

Further, our findings of correlations between phenology and other commonly measured traits highlight that accurate forecasts of future changes in phenology may benefit from accounting for the response of other traits to climate change. Across temperature and precipitation gradients, leaf size and shape, for example, also change, as species shift to conserve water and mitigate effects of transpiration under higher temperatures (De La Riva et al., 2016). These changes could impact species photosynthetic potential and ultimately ecosystem services, such as carbon sequestration. While phenological research has focused on forecasting responses to temperature, the correlation of other traits with photoperiod suggest its importance as a cue. It is therefore critical that we continue to take a more holistic approach to studying the relationships between phenology and plant traits to accurately forecast the future impacts of climate change on communities.

References

Albert, C. H., W. Thuiller, N. G. Yoccoz, A. Soudant, F. Boucher, P. Saccone, and S. Lavorel. 2010. Intraspecific functional variability: extent, structure and sources of variation. Journal of Ecology 98:604–613.

Basler, D., and C. Körner. 2014. Photoperiod and temperature responses of bud swelling and bud burst in four temperate forest tree species. Tree Physiology 34:377–388.

Cabon, A., L. Fernández-de-Uña, G. Gea-Izquierdo, F. C. Meinzer, D. R. Woodruff, J. Martínez-Vilalta, and M. De Cáceres. 2020. Water potential control of turgor-driven tracheid enlargement in Scots pine at its xeric distribution edge. New Phytologist 225:209–221.

Chave, J., D. Coomes, S. Jansen, S. L. Lewis, N. G. Swenson, and A. E. Zanne. 2009. Towards a worldwide wood economics spectrum. Ecology Letters 12:351–366.

Chuine, I. 2000. A unified model for budburst of trees. Journal of Theoretical Biology 207:337–347.

Chuine, I., X. Morin, and H. Bugmann. 2010. Warming, photoperiods, and tree phenology. Science 329:277–278.

Cleland, E. E., I. Chuine, A. Menzel, H. A. Mooney, and M. D. Schwartz. 2007. Shifting plant phenology in response to global change. Trends in Ecology and Evolution 22:357–365.

Cohen, J. M., M. J. Lajeunesse, and J. R. Rohr. 2018. A global synthesis of animal phenological responses to climate change. Nature Climate Change 8:224–228.

De La Riva, E. G., M. Olmo, H. Poorter, J. L. Ubera, and R. Villar. 2016. Leaf Mass per Area (LMA) and Its Relationship with Leaf Structure and Anatomy in 34 Mediterranean Woody Species along a Water Availability Gradient. PLOS ONE 11:e0148788.

Díaz, S., J. Kattge, J. H. C. Cornelissen, I. J. Wright, S. Lavorel, S. Dray, B. Reu, M. Kleyer, C. Wirth, I. Colin Prentice, E. Garnier, G. Bönisch, M. Westoby, H. Poorter, P. B. Reich, A. T. Moles, J. Dickie, A. N. Gillison, A. E. Zanne, J. Chave, S. Joseph Wright, S. N. Sheremet'ev, H. Jactel, C. Baraloto, B. Cerabolini, S. Pierce, B. Shipley, D. Kirkup, F. Casanoves, J. S. Joswig, A. Günther, V. Falczuk, N. Rüger, M. D. Mahecha, and L. D. Gorné. 2016. The global spectrum of plant form and function. Nature 529:167–171.

Finn, G. A., A. E. Straszewski, and V. Peterson. 2007. A general growth stage key for describing trees and woody plants. Annals of Applied Biology 151:127–131.

Flynn, D. F. B., and E. M. Wolkovich. 2018. Temperature and photoperiod drive spring phenology across all species in a temperate forest community. New Phytologist 219:1353–1362.

Gelman, A., J. Hill, and A. Vehtari. 2020. Regression and other stories. Cambridge University Press.

Green, S. J., C. B. Brookson, N. A. Hardy, and L. B. Crowder. 2022. Trait-based approaches to global change ecology: moving from description to prediction. Proceedings of the Royal Society B: Biological Sciences 289:20220071.

Grime, J. P. 1974. Vegetation classification by reference to strategies. Nature 250:26–31.

Gross, K. L., M. R. Willig, L. Gough, R. Inouye, and S. B. Cox. 2000. Patterns of species density and productivity at different spatial scales in herbaceous plant communities. Oikos 89:417–427.

Hawkins, B. A., B. Leroy, M. Á. Rodríguez, A. Singer, B. Vilela, F. Villalobos, X. Wang, and D. Zelený. 2017. Structural bias in aggregated species-level variables driven by repeated species co-occurrences: a pervasive problem in community and assemblage data. Journal of Biogeography 44:1199–1211.

Hoegh-Guldberg, O., D. Jacob, M. Taylor, M. Bindi, S. Brown, I. Camilloni, A. Diedhiou, R. Djalante, K. Ebi, F. Engelbrecht, J. Guiot, Y. Hijioka, S. Mehrotra, A. Payne, S. Seneviratne, A. Thomas, R. Warren, and G. Zhou. 2018. Impacts of 1.5 °C Global Warming on Natural and Human Systems. In: Global Warming of 1.5 °C. An IPCC Special Report on the impacts of global warming of 1.5 °C above pre-industrial levels and related global greenhouse gas emission pathways, in the context of . Tech. rep., Cambridge University Press, Cambridge, UK and New York, NY, USA.

Kang, M., S. X. Chang, E.-R. Yan, and X.-H. Wang. 2013. Trait variability differs between leaf and wood tissues across ecological scales in subtropical forests. Journal of Vegetation Science 25:703–714.

Kharouba, H. M., J. Ehrlén, A. Gelman, K. Bolmgren, J. M. Allen, S. E. Travers, and E. M. Wolkovich. 2018. Global shifts in the phenological synchrony of species interactions over recent decades. Proceedings of the National Academy of Sciences 115:5211–5216.

Körner, C., and D. Basler. 2010. Phenology Under Global Warming. Science 327:1461–1463.

Laube, J., T. H. Sparks, N. Estrella, J. Höfler, D. P. Ankerst, and A. Menzel. 2014. Chilling outweighs photoperiod in preventing precocious spring development. Global Change Biology 20:170–182.

Loughnan, D., F. A. Jones, G. Legault, C. J. Chamberlain, D. M. Buonaiuto, A. K. Ettinger, M. Garner, D. S. Sodhi, and E. M. Wolkovich. in prep. Woody plant phenological responses are strongly associated with key functional traits .

Loughnan, D., and E. M. Wolkovich. in prep. Temporal assembly of woody plant communities shaped equally by evolutionary history as by current environments .

McGill, B. J., B. J. Enquist, E. Weiher, and M. Westoby. 2006. Rebuilding community ecology from functional traits. Trends in Ecology and Evolution 21:178–185.

Menzel, A., T. H. Sparks, N. Estrella, E. Koch, A. Aaasa, R. Ahas, K. Alm-Kübler, P. Bissolli, O. Braslavská, A. Briede, F. M. Chmielewski, Z. Crepinsek, Y. Curnel, Å. Dahl, C. Defila, A. Donnelly, Y. Filella, K. Jatczak, F. Måge, A. Mestre, Ø. Nordli, J. Peñuelas, P. Pirinen, V. Remišová, H. Scheifinger, M. Striz, A. Susnik, A. J. Van Vliet, F. E. Wielgolaski, S. Zach, and A. Zust. 2006. European phenological response to climate change matches the warming pattern. Global Change Biology 12:1969–1976.

Messier, J., B. J. McGill, and M. J. Lechowicz. 2010. How do traits vary across ecological scales? A case for trait-based ecology. Ecology Letters 13:838–848.

Miller, J. E. D., E. I. Damschen, and A. R. Ives. 2019. Functional traits and community composition: A comparison among community-weighted means, weighted correlations, and multilevel models. Methods in Ecology and Evolution 10:415–425.

Parmesan, C., and G. Yohe. 2003. A globally coherent fingerprint of climate change impacts across natural systems. Nature 421:37–42.

Peres-Neto, P. R., S. Dray, and C. J. F. Ter Braak. 2017. Linking trait variation to the environment: critical issues with community-weighted mean correlation resolved by the fourth-corner approach. Ecography 40:806–816.

Pérez-Harguindeguy, N., S. Díaz, E. Garnier, S. Lavorel, H. Poorter, P. Jaureguiberry, M. S. Bret-Harte, W. K. Cornwell, J. M. Craine, D. E. Gurvich, C. Urcelay, E. J. Veneklaas, P. B. Reich, L. Poorter, I. J. Wright, P. Ray, L. Enrico, J. G. Pausas, A. C. de Vos, N. Buchmann, G. Funes,

F. Quétier, J. G. Hodgson, K. Thompson, H. D. Morgan, H. ter Steege, M. G. A. van der Heijden, L. Sack, B. Blonder, P. Poschlod, M. V. Vaieretti, G. Conti, A. C. Staver, S. Aquino, and J. H. C. Cornelissen. 2013. New handbook for standardized measurement of plant functional traits worldwide. Australian Journal of Botany 61:167–234.

Peters, R. L., K. Steppe, H. E. Cuny, D. J. De Pauw, D. C. Frank, M. Schaub, C. B. Rathgeber, A. Cabon, and P. Fonti. 2021. Turgor – a limiting factor for radial growth in mature conifers along an elevational gradient. New Phytologist 229:213–229.

Pollock, L. J., W. K. Morris, and P. A. Vesk. 2012. The role of functional traits in species distributions revealed through a hierarchical model. Ecography 35:716–725.

Primack, R. B., I. Ibáñez, H. Higuchi, S. D. Lee, A. J. Miller-Rushing, A. M. Wilson, and J. A. Silander. 2009. Spatial and interspecific variability in phenological responses to warming temperatures. Biological Conservation 142:2569–2577.

R Development Core Team. 2017. R: A language and environment for statistical computing.

Reich, P. B. 2014. The world-wide 'fast–slow' plant economics spectrum: a traits manifesto. Journal of Ecology 102:275–301.

Root, T. L., J. T. Price, K. R. Hall, S. H. Schneider, C. Rosenzweig, and J. A. Pounds. 2003. Fingerprints of global warming on wild animals and plants. Nature 421:57–60.

Schweingruber, F., and W. Landolt. 2010. The xylem database.

Shipley, B., F. De Bello, J. H. C. Cornelissen, E. Laliberté, D. C. Laughlin, and P. B. Reich. 2016. Reinforcing loose foundation stones in trait-based plant ecology. Oecologia 180:923–931.

Stan Development Team. 2018. RStan: the R interface to Stan. R package version 2.17.3.

Standen, K. M., and J. Baltzer. 2023. Greater variation in boreal plant community composition and community-level traits at local-than regional-scale. Journal of Vegetation Science 34:1–14.

Thackeray, S. J., P. A. Henrys, D. Hemming, J. R. Bell, M. S. Botham, S. Burthe, P. Helaouet, D. G. Johns, I. D. Jones, D. I. Leech, E. B. MacKay, D. Massimino, S. Atkinson, P. J. Bacon, T. M. Brereton, L. Carvalho, T. H. Clutton-Brock, C. Duck, M. Edwards, J. M. Elliott, S. J. Hall, R. Harrington, J. W. Pearce-Higgins, T. T. Høye, L. E. Kruuk, J. M. Pemberton, T. H. Sparks, P. M. Thompson, I. White, I. J. Winfield, and S. Wanless. 2016. Phenological sensitivity to climate across taxa and trophic levels. Nature 535:241–245.

Violle, C., M. Navas, D. Vile, E. Kazakou, C. Fortunel, I. Hummel, and E. Garnier. 2007. Let the concept of trait be functional! Oikos 116:882–892.

Wiemann, M. C., and W. G. Bruce. 2002. Geographic variation in wood specific gravity: effects of latitude, temperature, and preciptitation. Wood and Fiber Science 34:96–107.

Wright, I. J., M. Westoby, P. B. Reich, J. Oleksyn, D. D. Ackerly, Z. Baruch, F. Bongers, J. Cavender-Bares, T. Chapin, J. H. C. Cornellissen, M. Diemer, J. Flexas, J. Gulias, E. Garnier, M. L. Navas, C. Roumet, P. K. Groom, B. B. Lamont, K. Hikosaka, T. Lee, W. Lee, C. Lusk, J. J. Midgley, Ü. Niinemets, H. Osada, H. Poorter, P. Pool, E. J. Veneklaas, L. Prior, V. I. Pyankov, S. C. Thomas, M. G. Tjoelker, and R. Villar. 2004. The worldwide leaf economics spectrum. Nature 428:821–827.

Wright, J. P., A. S. Flecker, and C. G. Jones. 2003. Local vs. landscape controls on plant species richness in Beaver meadows. Ecology 84:3162–3173.

Zohner, C. M., B. M. Benito, J.-C. Svenning, and S. S. Renner. 2016. Day length unlikely to constrain climate-driven shifts in leaf-out times of northern woody plants. Nature Climate Change 6:1120–1123.

Figures

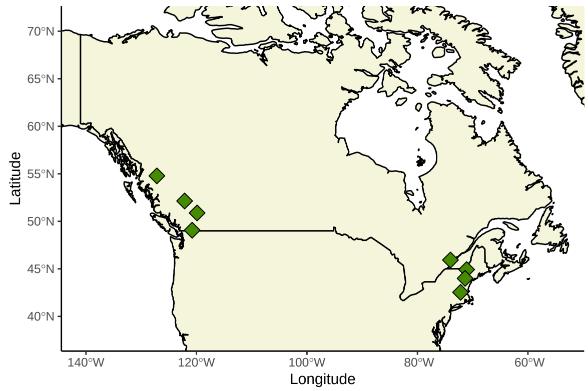

Figure 1: We measured leaf and structural traits in eight temperate deciduous forests, spanning four eastern populations and four western population, across a latitudinal gradients of 4-6°. The branch clippings used in our two growth chamber experiments were taken from the most northern and most southern populations in each transect.

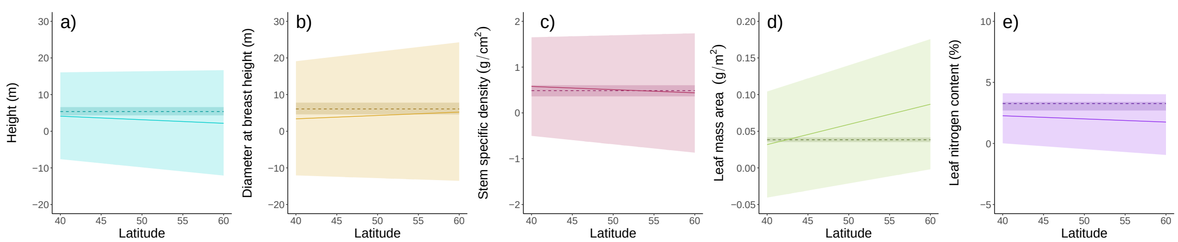

Figure 2: We found geographic differences for only one of our functional traits, the majority exhibiting no differences between latitudes or across transects. Depicted are the spatial trends for, a. height, b. diameter at base height, c. stem specific density, d. leaf mass area, and e. leaf nitrogen content. Dashed lines represent the western transect and solid lines the eastern transect.

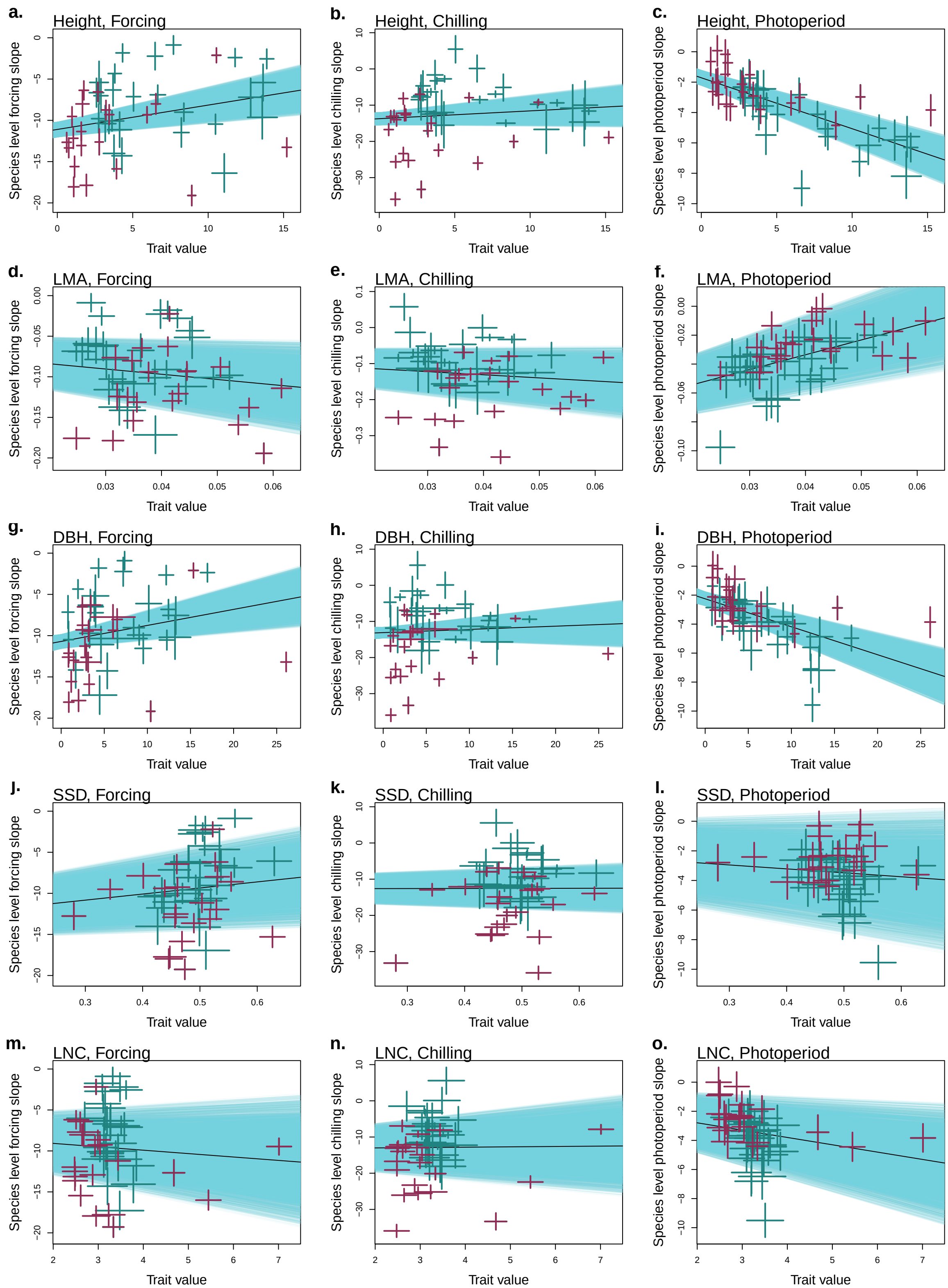

Figure 3: Relationships between species traits and cue responses showed considerable variation across a-c. height, d-f. leaf mass area, g-i. diameter at breast height, j-l. stem specific density, and m-o. the leaf nitrogen content. Point colours representing different species groups, with tree species are depicted in maroon and shrub species in teal. The blue band depicts the 90% uncertainty interval.

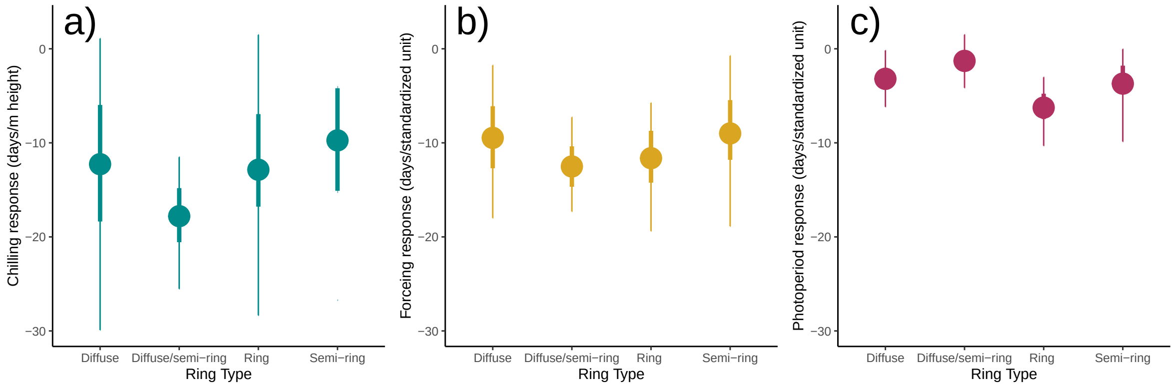

Figure 4: Despite species wood structures causing differing growth strategies in the spring, we did not find this trait to correlate with differences in cues across species. Thinner lines represent the 90% UI and thicker lines the 50% UI. Here we show the correlation using the posterior estimates from the height model only, but trends were consistent across all traits (Table 2-5).

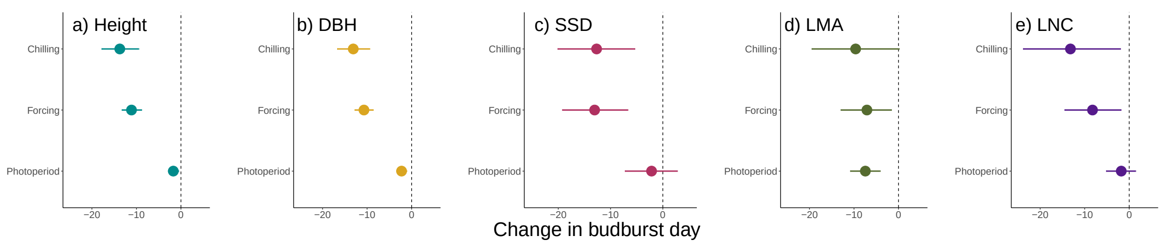

Figure 5: We found fairly consistent estimates for budburst cue responses to chilling, forcing, and photoperiod for each of our trait models: a. height, b. diameter at breast height, c. stem specific density, d. leaf mass area, and e. leaf nitrogen contnet. Lines represent 90% uncertainty intervals and points the mean estimate.

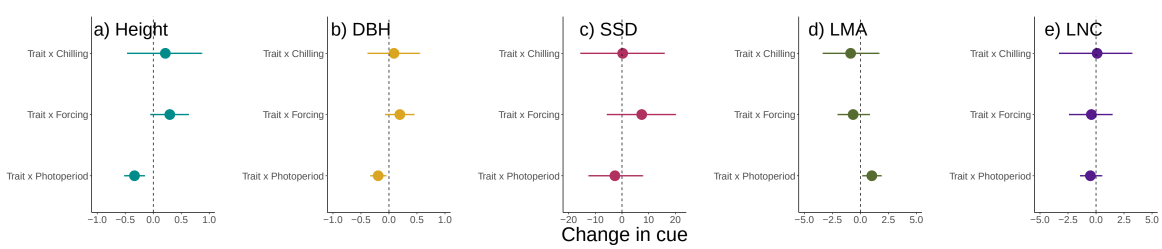

Figure 6: The relationships between traits and cue responses varied considerably across each of our trait models, a. height, b. diameter at breast height, c. stem specific density, d. leaf mass area, and e. leaf nitrogen content, and for individual cues. Lines represent 90% uncertainty intervals and points the mean estimate. Note the differences in the scale of the x-axis.

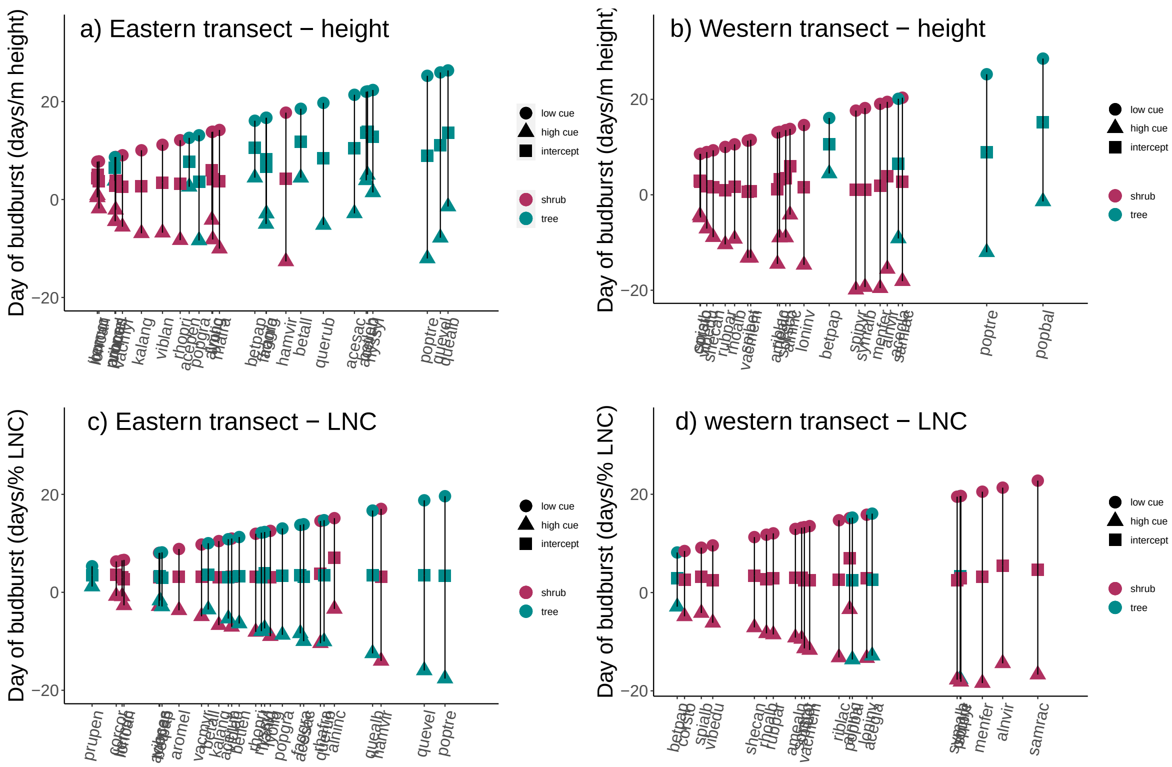

Figure 7: We found budburst estimates differed between our full model (intercept plus cues, depicted as triangles for high cues and as circles for low cues), versus the intercepts only model (without cues, shown as squares). Species are ordered in increasing budburst dates for both the eastern (a & c) and western (b & d) populations, spanning from early budbursting shrubs, in red, to late budbursting trees in blue. For traits such as height (a & b) we found distinct partitioning of budburst across shrub and tree species, but this was not the case for all traits, with our model of leaf nitrogen content showing highly mixed budburst order of shrub and tree species (c & d).

490 # Tables

Table 1: Summary output from a joint Bayesian model of height and budburst phenology in which species are partially pooled. The effect of transect is modeled as a categorical variable and latitude as continuous in its interaction term with transect. The model includes environmental cues as z-scored continuous variables, allowing comparisons to be made across cues.

	mean	5%	25%	75%	95%
Transect	2.60	-3.00	0.40	4.90	8.30
Transect x latitude	-0.10	-0.20	-0.10	-0.00	0.00
Forcing	-11.10	-13.30	-12.00	-10.20	-8.80
Chilling	-13.70	-17.80	-15.50	-12.10	-9.50
Photoperiod	-1.70	-2.90	-2.20	-1.20	-0.50
Trait x forcing	0.30	-0.10	0.20	0.40	0.60
Trait x chilling	0.20	-0.50	-0.00	0.50	0.90
Trait x photoperiod	-0.30	-0.50	-0.40	-0.30	-0.20

Table 2: Summary output from a joint Bayesian model of DBH and budburst phenology in which species are partially pooled. The effect of transect is modeled as a categorical variable and latitude as continuous in its interaction term with transect. The model includes environmental cues as z-scored continuous variables, allowing comparisons to be made across cues

	mean	5%	25%	75%	95%
Transect	-6.40	-13.70	-9.40	-3.40	1.00
Transect x latitude	0.10	-0.10	0.00	0.20	0.30
Forcing	-10.70	-12.80	-11.60	-9.90	-8.60
Chilling	-13.10	-16.70	-14.60	-11.60	-9.40
Photoperiod	-2.30	-3.40	-2.70	-1.80	-1.10
Trait x forcing	0.20	-0.10	0.10	0.30	0.40
Trait x chilling	0.10	-0.40	-0.10	0.30	0.50
Trait x photoperiod	-0.20	-0.30	-0.20	-0.10	-0.10

Table 3: Summary output from a joint Bayesian model of SSD and budburst phenology in which species are partially pooled. The effect of transect is modeled as a categorical variable and latitude as continuous in its interaction term with transect. The model includes environmental cues as z-scored continuous variables, allowing comparisons to be made across cues.

	mean	5%	25%	75%	95%
Transect	0.40	-0.10	0.20	0.60	0.90
Transect x latitude	-0.00	-0.00	-0.00	-0.00	0.00
Forcing	-13.00	-19.30	-15.70	-10.50	-6.70
Chilling	-12.70	-20.10	-15.60	-9.70	-5.40
Photoperiod	-2.20	-7.20	-4.20	-0.00	2.80
Trait x forcing	7.40	-5.70	2.00	13.00	20.10
Trait x chilling	0.30	-15.60	-5.90	6.50	15.90
Trait x photoperiod	-2.70	-12.60	-7.00	1.50	7.80

Table 4: Summary output from a joint Bayesian model of LMA and budburst phenology in which species are partially pooled. The effect of transect is modeled as a categorical variable and latitude as continuous in its interaction term with transect. The model includes environmental cues as z-scored continuous variables, allowing comparisons to be made across cues.

	mean	5%	25%	75%	95%
Transect	-11.70	-15.30	-13.20	-10.20	-8.00
Transect x latitude	0.30	0.20	0.20	0.30	0.40
Forcing	-7.10	-13.00	-9.30	-4.80	-1.60
Chilling	-9.60	-19.50	-13.50	-5.70	0.20
Photoperiod	-7.50	-10.90	-8.90	-6.00	-4.10
Trait x forcing	-0.60	-2.00	-1.20	-0.10	0.80
Trait x chilling	-0.90	-3.40	-1.90	0.10	1.70
Trait x photoperiod	1.00	0.20	0.70	1.40	1.90

Table 5: Summary output from a joint Bayesian model of LNC and budburst phenology in which species are partially pooled. The effect of transect is modeled as a categorical variable and latitude as continuous in its interaction term with transect. The model includes environmental cues as z-scored continuous variables, allowing comparisons to be made across cues.

	mean	5%	25%	75%	95%
Transect	0.00	-0.80	-0.30	0.40	0.90
Transect x latitude	-0.00	-0.00	-0.00	-0.00	-0.00
Forcing	-8.20	-14.50	-10.80	-5.80	-1.80
Chilling	-13.20	-23.80	-17.70	-8.80	-2.00
Photoperiod	-1.80	-5.20	-3.10	-0.40	1.40
Trait x forcing	-0.40	-2.40	-1.20	0.40	1.40
Trait x chilling	0.10	-3.30	-1.20	1.50	3.20
Trait x photoperiod	-0.50	-1.40	-0.90	-0.10	0.50